Journal of Materials Chemistry C

ROYAL SOCIETY OF CHEMISTRY

PAPER

View Article Online
View Journal | View Issue

Cite this: J. Mater. Chem. C, 2024, 12, 941

Color-tunable light-emitting fibers for pattern displaying textiles†

Peiyu Liu,‡[a] Yang Xiang,‡[a] Yue Liu,[a] Sunny Shulei Peng,[b] Zhengfeng Zhu,[a] Xiang Shi,[a] Jingxia Wu*[a] and Peining Chen *[a]

Received 3rd November 2023,
Accepted 4th December 2023

DOI: 10.1039/d3tc04009g

rsc.li/materials-c

Flexible displays for visual transmission and interaction are indispensable in wearable electronics. Color-tunable light-emitting fibers (CLFs) with wide gamut are promising candidates to realize full-color pattern displaying for smart electronic textiles, but have not been reported yet. Herein, thousands of meters of color-tunable light-emitting fibers with multilayer coaxial structure are fabricated by a facile step-by-step solution deposition process. Real-time color tuning is achieved by mixing luminescent spectra from ZnS:Cu and ZnS:Mn phosphor layers with different dielectric constants under external electric fields. The CLFs could emit colors from orange, white, blue to blue-violet by varying the applied voltages. The luminescence performances of the light-emitting fibers are well maintained under long-term high temperature and ultra-violet radiation tests, and after 10 000 cycles of folding deformation. The luminescence intensity varied less than 10% along the fiber with an investigated length of 100 meters. These light-emitting fibers are precisely woven into smart electronic textiles displaying desirable colorful patterns.

1. Introduction

Electronic textiles with functions of energy harvesting,[1–3] energy supplying[4–6] and sensing[7–9] are promising in various fields, such as wearable electronics, the Internet of Things and smart healthcare. As the basic building blocks of electronic textile systems, textiles with displaying capacity are urgently needed to satisfy the increasing demands for convenient human-machine interaction experiences.[10–14] A mainstream strategy to build displaying textiles is directly weaving light-emitting fibers into textiles with designed patterns.[15–17] Such displaying textiles could achieve desired text or picture playing by combining with appropriate control circuits. Recently, various light-emitting fibers with different emitting colors have been made,[18–21] but the real-time color-tunning capacity with a wide color gamut remains an unmet need, making it difficult to effectively satisfy the full-color displaying requirements of electronic textile systems.

Currently, numerous luminescent materials can be used to fabricate light-emitting fibers, including organic and inorganic materials.[22–27] Organic light-emitting fibers typically require rigorous preparation conditions and encapsulation to prevent device failure.[13,28,29] In comparison, light-emitting fibers based on inorganic materials, such as ZnS phosphor materials, have been widely explored due to the facile processing process for the luminescent functional layer and good stability for practical applications.[30,31] Specifically, ZnS phosphor-based light-emitting fibers are generally fabricated with a simple structure by assembling phosphor materials incorporated with a dielectric polymer onto the conductive fibers,[11,32,33] and then covering with a transparent conductive layer as the external electrode.[18,30,34] The light emission mechanism of such fibers relies on the radiative relaxation of the luminescent center under an alternating electric field.[35] However, their luminescent spectral range greatly depends on the types of doped activators in ZnS phosphors.[36] For instance, ZnS phosphors doped with Cu and Mn activators only emit blue and orange light, respectively, nearly unchanged under different electric field intensities. That is, current light-emitting fibers based on ZnS phosphors generally emit light with relatively simple color, making it hard to meet the colorful displaying requirements for electronic textile systems.

Here, we present flexible and color-tunable light-emitting fibers (CLFs) by designing double-stacked emitting layers with different dielectric constants. Thousands of meters of color-tunable light-emitting fibers with multilayer coaxial structures are fabricated by a facile step-by-step solution deposition process. They could achieve light emission with various colors

[a] State Key Laboratory of Molecular Engineering of Polymers, Department of Macromolecular Science, Institute of Fiber Materials and Devices, and Laboratory of Advanced Materials, Fudan University, Shanghai, 200438, China. E-mail: wujingxia@fudan.edu.cn, peiningc@fudan.edu.cn

[b] High School Affiliated to Fudan University, Qingpu Campus, Shanghai, 201700, China

† Electronic supplementary information (ESI) available. See DOI: https://doi.org/10.1039/d3tc04009g

‡ The first two authors contributed equally to this work.

by varying the electric field intensity, combined with a wide color gamut from orange, to white to blue. The luminance and color gamut of color-tunable light-emitting fibers are well maintained under high temperature (95 °C for one week) and after repeated folding deformations for 10 000 cycles, demonstrating good flexibility and mechanical stability. These color-tunable light-emitting fibers are precisely woven into textiles to form a peony pattern, realizing colorful displays for efficient human-machine interactions.

2. Experimental section

Materials

Silver-plated nylon yarns (100D, Hengtong X-silver Specialty Textile Co., Ltd) were used as an inner conductive fiber electrode. $BaTiO_3$ (Shanghai DianYang Industry Co., Ltd) was used as an inorganic dielectric material, ZnS:Mn and ZnS:Cu phosphors (Shanghai Keyan Phosphor Technology Co., Ltd) were employed as luminescent materials. Waterborne polyurethane (Shanghai Sisheng Polymer Materials Co., Ltd) and FR (Daikin Fluorochemicals Co., Ltd) were utilized as a polymer matrix. *N*,*N*-Dimethylformamide (DMF, Sinopharm) was used as a solvent for FR.

Preparation of a dielectric layer

The dielectric composites were prepared by dispersing $BaTiO_3$ particles into 12.5 wt% FR/DMF solution, and the mass ratio of barium titanate to solution was 3 : 1. The silver-plated nylon compound yarns (100D) were dipped into the dielectric precursor dispersion and pulled out at a speed of 10 m min^{-1} through a homemade die (with a diameter of 175 μm). The fiber was then dried in a two-meter-long oven at 180 °C.

Preparation of light-emitting fibers

The phosphor precursor dispersions were prepared by mixing ZnS:Mn phosphors and ZnS:Cu phosphors with different weight ratios in polyurethane aqueous dispersion and FR/DMF solution. The inner conductive fiber electrode with a dielectric layer was firstly dipped with ZnS:Cu phosphor dispersion with different weight ratios through homemade dies at a speed of 8 m min^{-1}. The fiber with a blue emitting layer was dipped with ZnS:Mn phosphor dispersion with different weight ratios through homemade dies at a speed of 8 m min^{-1}. The prepared fibers were then dried in a two-meter-long oven at 180 °C to remove solvents. The Ag nanowire dispersion was then coated around the fiber surface as the outer electrode. The copper wire could be further wound around the fiber to further enhance the conductivity of the outer electrode.

Characterization

The morphology of the ZnS phosphors and the devices was collected by a field emission scanning electron microscope (S-4800, Hitachi) operating at 1 kV; the cross-sectional geometry of the devices was collected by a fluorescence microscope (BX51, Olympus); the photographs were taken by a digital camera (α6000, Sony); the luminescent color characteristics (luminance, luminescence spectrum, and CIE coordinates) of the devices were excited with an amplifier (ATA-2081, Aigtek) and a functional waveform generator (3300B, Keysight). The data were collected with a spectroscopic spectrometer (PR680, Photoresearch). The ultraviolet (UV) simulation tests were carried out under a UV lamp aging chamber (YNK/UVA-340, Suzhou Unik Environmental Testing Equipment Co., Ltd); the high-temperature tests were carried out under a vacuum drying chamber (25 L) at 95 °C (DZF-6020, Hefei Kejing Material Technology Co., Ltd), and the bending tests were conducted in a flexible electronic tester (FT2000, Shanghai Power Square Electronic Technology Co., Ltd). The electric field distribution was modeled with the finite element software COMSOL to simulate the electric field distribution of a device with a dielectric layer and a double layer of light emitting layers. In the 3D model, each layer was reduced to a homogeneous dielectric or conductor.

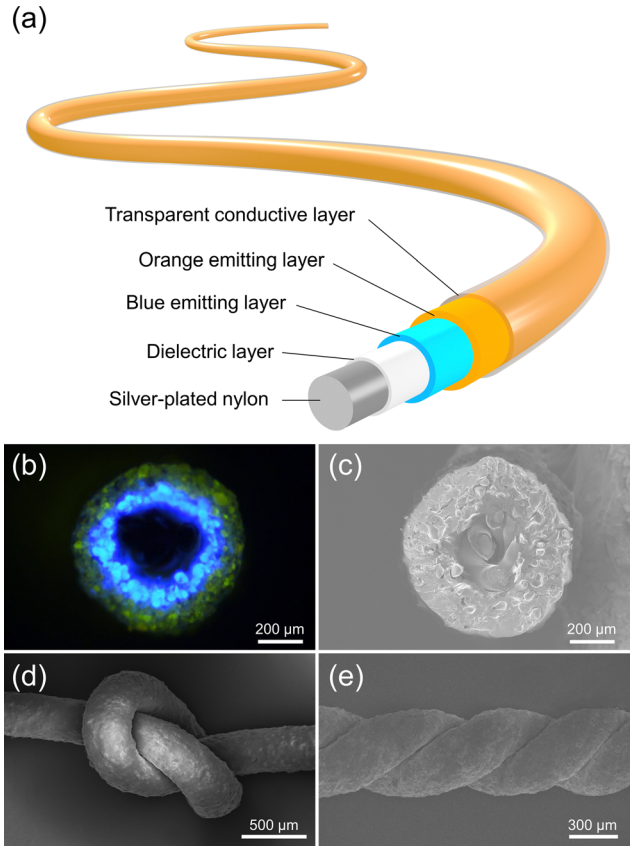

Fig. 1 The design and structural characterization of the CLFs. (a) Schematic illustrating the structure design of the CLFs. (b) Cross-sectional fluorescence image of CLFs. (c) Cross-sectional SEM image of CLFs. (d) SEM image of knotted CLFs. (e) SEM image of the twisted CLFs.

3. Results and discussion

Typically, the CLFs had a core-sheath structure, consisting of an inner conductive fiber electrode, a dielectric layer, double-stacked emitting layers, and an outer conductive layer (Fig. 1a). Specifically, the dielectric layer was made of FR matrix

incorporated with $BaTiO_3$ nanoparticles (Fig. S1 (ESI†)).[37] The double-stacked emitting layer of CLFs was fabricated by sequentially dip coating ZnS:Cu phosphors/FR and ZnS:Mn phosphors/PU dispersions (Fig. S2–S4 (ESI†)). The resultant ZnS:Cu phosphors/FR and ZnS:Mn phosphors/PU layers had the same thickness of 50 μm and were uniform along the fiber length direction (Fig. 1b and Fig. S5, (ESI†)). ZnS:Cu phosphors were uniformly mixed in fluorine rubber with high dielectric constant to serve as a blue emitting layer, while ZnS:Mn phosphors were uniformly mixed in polyurethane with low dielectric constant to serve as an orange emitting layer. These two light-emitting layers were in intimate contact with each other, and no obvious gaps were observed between them (Fig. 1c). Moreover, as shown in Fig. S6 (ESI†), the transparent conductive layer made of Ag nanowires was uniformly coated around the curved fiber surface, where the Ag nanowires were interconnected with each other to form a transparent conductive network.[18,38,39] The resultant CLFs were structurally stable to withstand various deformations, and no surface/interface cracks had occurred as they were knotted or twisted (Fig. 1d and e). By using this preparation method, other solution-processable luminescent materials like zinc cadmium sulfide selenide, strontium sulfide and calcium sulfide could also be deposited onto the fiber substrate to fabricate CLFs.

The light-emitting behaviors of CLFs were investigated by applying alternating electric fields to inner and outer electrodes (Fig. 2a). The color-tunable light emission mainly resulted from the different electric field distribution in the ZnS:Cu phosphors/FR and ZnS:Mn phosphors/PU layers.[40] The dielectric constant of FR is much higher than that of PU,[40] and thus the electric field strength in the orange layer consisting of Zn:Mn phosphors/PU was higher than that in the blue layer consisting of ZnS:Cu phosphors/FR. By adjusting the applied voltage, the relative luminescent brightness of the two light-emitting layers could be tuned to emit light with desired colors through the light mixture. Through simulating the distribution of the electric field, the electric field was strongly concentrated on the orange emitting layer with a lower dielectric constant under

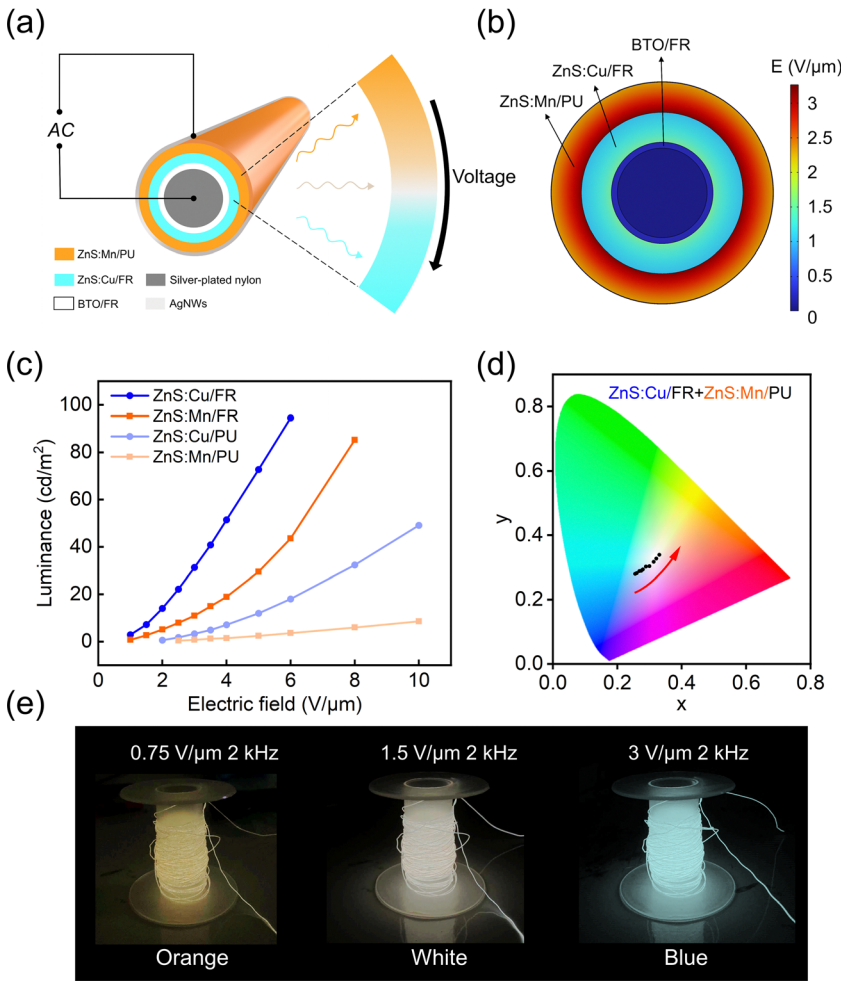

Fig. 2 Light-emitting performances of the CLFs. (a) Schematic to show the operating principle of the CLFs. (b) Simulation of electric field distribution of CLFs composed with ZnS:Cu/FR and ZnS:Mn/PU light-emitting layers. (c) Luminance of the CLFs with a single-light-emitting layer (ZnS:Cu/FR, ZnS:Cu/PU, ZnS:Mn/FR and ZnS:Mn/PU) at varied electric field intensity. (d) CIE coordinates of CLFs with a single-light-emitting layer (ZnS:Cu/FR and ZnS:Mn/PU) at varied electric field intensity. (e) Photographs of the CLFs showing color changes from orange to white to blue at different applied electricity.

the applied voltage (Fig. 2b). However, the intrinsic luminescent properties of the two kinds of ZnS phosphors also contributed to the color-tuning light emitting behaviors. In the same polymer, the luminance intensity of the ZnS:Cu increased more rapidly with enhanced voltage compared to ZnS:Mn (Fig. 2c). Therefore, the orange light (peak emission at 586 nm) emitted from ZnS:Mn became dominant at a low applied voltage, due to the higher electric field strength in the orange layer than in the blue layer. However, the blue light (peak emission at 458 nm) emitted from ZnS:Cu gradually became dominant with the increase of the applied voltage, because its steep luminescence-voltage curve exhibited strong intensity of blue light even under low electric field strength. To avoid shading the orange emission with lower intensity and thus influencing the color gamut of CLFs, the orange emitting layer was designed above the blue emitting layer. As shown in the Commission Internationale de l'Eclairage (CIE) coordinate, multicolor lights such as orange, white and blue could be achieved (Fig. 2d). Upon varying the applied alternating electric voltages, the 100-meter-long CLFs showed distinct luminescent colors (Fig. 2e), ranging from orange (0.75 V μm^{-1}, 2 kHz) and white (1.5 V μm^{-1}, 2 kHz) to blue (2 V μm^{-1}, 2 kHz).

The color-tuning capacities (color gamut) of the light-emitting fibers at different parameters were carefully studied. When the content of the two phosphors was 1 : 1, the CLFs with a 50-μm-thickness light-emitting layer showed the widest color gamut, and their CIE coordinates varied from (0.3644, 0.3656) to (0.2749, 0.2968), as shown in Fig. S7 (ESI†). In addition, the light-emitting fibers with diverse phosphor content in a double-stacked emitting layer were also studied. When the weight ratio of ZnS:Cu phosphors and ZnS:Mn phosphors was 1 : 1.5, the light-emitting fibers exhibited the widest color gamut, and their CIE coordinates varied from (0.3927, 0.3986) to (0.2771, 0.3004), as shown in Fig. S8 and S9 (ESI†). Furthermore, the light-emitting fibers with disparate relative thickness of the two emitting layers were further analyzed. When the thicknesses of the blue-emitting and orange-emitting layers were both 50 μm, the CLFs emitted changeful light with the widest color gamut, and their CIE coordinates varied from (0.3883, 0.375) to (0.2634, 0.2976), as shown in Fig. S10 (ESI†).

For comparison, the light emitting behaviors of the other two kinds of counterpart fibers were carefully studied. For the single-light-emitting-layer fibers by mixing ZnS:Cu and ZnS:Mn phosphors in a PU matrix (with a weight ratio of 1 : 1), the blue light (with peak emission of 458 nm) generated by ZnS:Cu phosphors was dominated in the spectrum, as shown in Fig. S11a (ESI†). There was no obvious change for the shape of the EL spectra and the position of the CIE coordinates, because the two kinds of phosphors were assigned the same electric field strength in the same layer. Therefore, the device containing a single light-emitting layer with mixed color phosphors could not exhibit multicolor light emission, as shown in Fig. S11b and c (ESI†). For the light-emitting fibers with double emitting layers using ZnS:Cu phosphors/PU as a blue emitting layer, and ZnS:Mn phosphors/FR as an orange emitting layer, by varying the electric fields, the spectrum was dominant with

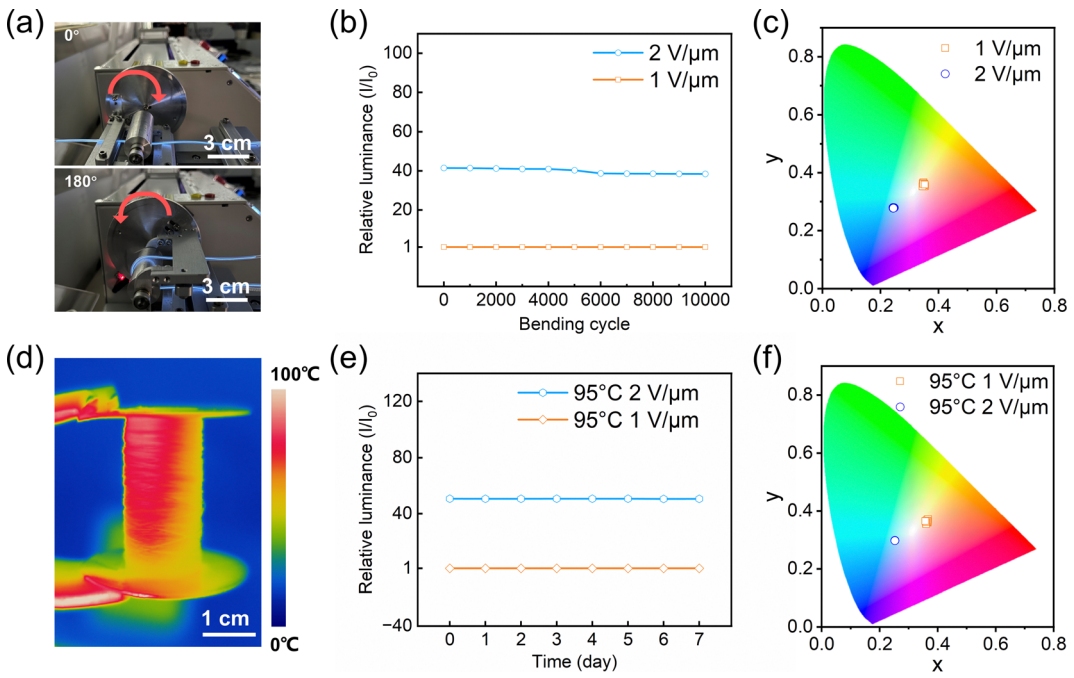

Fig. 3 Stability and durability of the CLFs. (a) Photographs of CLFs being bent with different angles. (b) Relative luminance of the CLFs with a double-light-emitting layer (ZnS:Cu/FR and ZnS:Mn/PU) after 10 000 bending cycles at an electric field intensity of 2 V μm^{-1} and 1 V μm^{-1}. The frequency was 2 kHz. (c) CIE coordinates of CLFs at electric fields of 2 V μm^{-1} and 1 V μm^{-1}. (d) Infrared thermal image of a spool of CLFs under temperatures of 95 °C. (e) and (f) Relative luminance and CIE coordinates of the CLFs under temperatures of 95 °C for 7 days. The applied electric fields were 2 V μm^{-1} and 1 V μm^{-1}, and the frequency was 2 kHz.

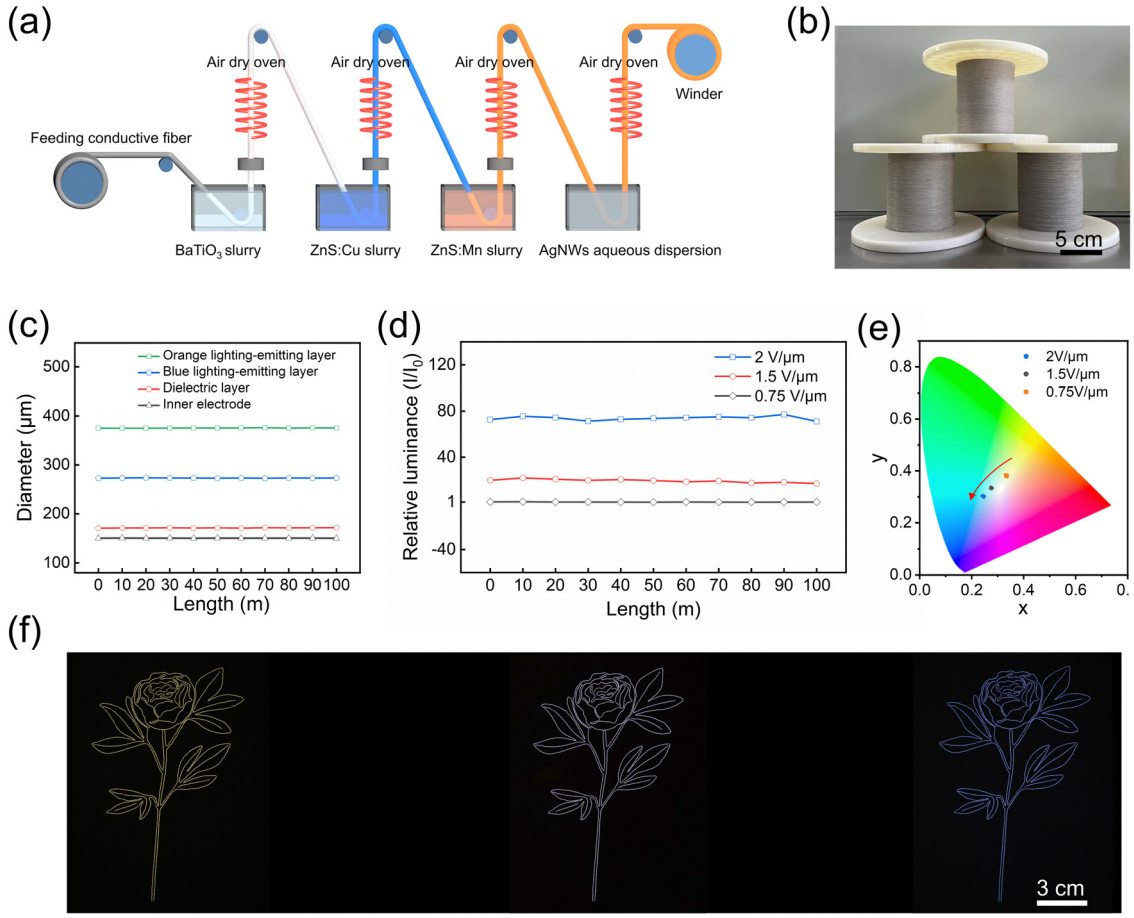

Fig. 4 Continuous fabrication and application demonstration of CLFs. (a) Schematic illustration of the continuous fabrication process of CLFs. (b) Photograph of spools of CLFs with a length of thousands of meters. (c) The consistency of the diameters of the inner electrode, dielectric layer, blue lighting-emitting layer and orange lighting-emitting layer for a 100-meter-long CLF. (d) and (e) Relative luminance and corresponding CIE coordinates of CLFs with double-light-emitting layers (ZnS:Cu/FR and ZnS:Mn/PU) for 100-meter-long CLFs. (f) Photographs of the light-emitting and colorful peony pattern embroidered with CLFs.

blue light, and the EL spectra and corresponding CIE coordinates were nearly unchanged, as shown in Fig. S12a and b (ESI†), indicating that the color tuning in this case was also unavailable. The simulation results of the electric field distribution further confirmed that the electric field intensity assigned to the blue emitting layer was dominant, as shown in Fig. S12c (ESI†). That is, the intensity of the electric field for the ZnS:Mn phosphors was not high enough to emit orange light and mix with blue light. As a result, the brightness of the blue light exceeded that of the orange light under different electric field intensities.

Flexibility and stability are critical for CLFs to withstand complex deformations during the weaving process and practical wearable use. The luminance of the CLFs remained stable when they were bent at the angles from 0° to 180° (Fig. 3a). Furthermore, with a bending angle of 180°, the luminance of the CLFs was maintained at 94% of the initial value after bending for 10 000 cycles (Fig. 3b), and exhibited no obvious variation in the CIE coordinates (Fig. 3c). Accordingly, the interfaces among the functional layers in the CLFs remained stable after cyclic bending deformations, thus ensuring that no short circuit or electrical breakdown occurred. Moreover, the tensile strength and breaking elongation of the CLFs were 95.2 MPa and 25.9%, respectively (Fig. S13 (ESI†)), which is similar to that of traditional polyester fibers. The luminescence performances of the CLFs were well maintained even under repeated stretching and compressing deformations (Fig. S14 and S15 (ESI†)). The CLFs could also be stably operated under high temperature. The luminance (varied by less than 10%) and the CIE coordinates were well maintained at a high temperature of 95 °C for 7 days (Fig. 3d–f). In addition, the device exhibited excellent stability during durable long-term ultraviolet radiation tests. Under a temperature of 60 °C and a radiation intensity of 1.1 W m^{-2}, the luminance and CIE coordinates of the CLFs were nearly unchanged after 7 days of radiation test, as shown in Fig. S16 (ESI†).

The CLFs could be continuously fabricated at a length of thousands of meters through a step-by-step solution deposition process. Compared with the in-situ synthesis of luminescence materials on the fiber electrode, the direct deposition process is simpler and easier for scalable preparation. We designed homemade coating-drying equipment to ensure the uniformity of each functional layer in the longitudinal and circumferential

directions (Fig. 4a), and Fig. 4b shows the CLFs continuously collected on the reels at a large scale. The diameter of the 100-meter-long CLFs was nearly unchanged as the length increased (Fig. 4c). We defined $C = (W - N)/(W + N)$ as the parameter of coaxiality, where the values of W and N represented the maximum and minimum diameters of the functional layers. The resulting C values of both the blue and orange emission layers were around 0.01 and well maintained, indicating the high coaxiality of the functional layers and the feasibility of the preparation process, as shown in Fig. S17 (ESI†). As shown in Fig. 4d and e, the luminance and emitting color demonstrated high consistency when CLFs were measured every 10 meters. To demonstrate the displaying capability in the textile, we embroidered CLFs into a traditional cotton textile through the rope embroidery process to create a colorful peony displaying pattern. Under different driving electricity, the luminescent colors of the peony pattern were changed from orange, to white, to blue continuously (Fig. 4f), demonstrating the potential of CLFs in displaying applications for smart electronic textiles.

4. Conclusions

In summary, a color-tunable light-emitting fiber was made by designing double light-emitting layers with different dielectric constants. Such CLFs could be fabricated continuously by a facile step-by-step solution coating method. The color-tunable capacity of the CLFs could be controlled by external electric fields to achieve wide-gumnut colors from orange to white to blue. The mechanism of color tuning was attributed to the electric field difference in the light-emitting layers with varied dielectric constants. The resultant CLFs demonstrated stable luminescent and color-tunable performances under complex deformations, high temperature and ultra-violet radiation. They were woven into textiles to obtain dynamic and colorful pattern displaying for convenient human-machine interactions.

Author contributions

Peiyu Liu: data curation, formal analysis, investigation, writing original draft. Yang Xiang: data curation, formal analysis, investigation, writing original draft. Yue Liu: data curation, formal analysis, investigation, writing-review & editing. Sunny Shulei Peng: investigation, writing-review & editing, validation. Zhengfeng Zhu: methodology, writing-review & editing, validation. Xiang Shi: methodology, writing-review & editing. Jingxia Wu: conceptualization, visualization, writing-review & editing. Peining Chen: conceptualization, supervision, writing-review & editing.

Conflicts of interest

There are no conflicts to declare.

Acknowledgements

This work was supported by MOST (2022YFA1203001, 2022YFA1203002) and NSFC (T2222005, 22175042).

References

1 Z. Zhu, Z. Lin, W. Zhai, X. Kang, J. Song, C. Lu, H. Jiang, P. Chen, X. Sun, B. Wang, Z. Wang and H. Peng, *Adv. Mater.*, 2023, e2304876, DOI: **10.1002/adma.202304876**.
2 S. S. Kwak, H. J. Yoon and S. W. Kim, *Adv. Funct. Mater.*, 2019, **29**, 1970011.
3 Z. Chai, N. Zhang, P. Sun, Y. Huang, C. Zhao, H. Fang, X. Fan and W. Mai, *ACS Nano*, 2016, **10**, 9201–9207.
4 J. He, C. Lu, H. Jiang, F. Han, X. Shi, J. Wu, L. Wang, T. Chen, J. Wang, Y. Zhang, H. Yang, G. Zhang, X. Sun, B. Wang, P. Chen, Y. Wang, Y. Xia and H. Peng, *Nature*, 2021, **597**, 57–63.
5 M. Liao, C. Wang, Y. Hong, Y. Zhang, X. Cheng, H. Sun, X. Huang, L. Ye, J. Wu, X. Shi, X. Kang, X. Zhou, J. Wang, P. Li, X. Sun, P. Chen, B. Wang, Y. Wang, Y. Xia, Y. Cheng and H. Peng, *Nat. Nanotechnol.*, 2022, **17**, 372–377.
6 S. Xu, Y. Yao, Y. Guo, X. Zeng, S. Lacey, H. Song, C. Chen, Y. Li, J. Dai, Y. Wang, Y. Chen, B. Liu, K. Fu, K. Amine, J. Lu and L. Hu, *Adv. Mater.*, 2018, **30**, 1704907.
7 W. Zhong, W. Liu, Y. Ke, K. Jia, X. Ming, M. Li, D. Wang, Y. Chen and H. Jiang, *J. Mater. Chem. C*, 2023, **11**, 14796–14804.
8 L. Shuai, Z. Guo, P. Zhang, J. Wan, X. Pu and Z. Wang, *Nano Energy*, 2020, **78**, 105389.
9 S. Seyedin, S. Uzun, A. Levitt, B. Anasori, G. Dion, Y. Gogotsi and J. M. Razal, *Adv. Funct. Mater.*, 2020, **30**, 1910504.
10 X. Shi, Y. Zuo, P. Zhai, J. Shen, Y. Yang, Z. Gao, M. Liao, J. Wu, J. Wang, X. Xu, Q. Tong, B. Zhang, B. Wang, X. Sun, L. Zhang, Q. Pei, D. Jin, P. Chen and H. Peng, *Nature*, 2021, **591**, 240–245.
11 S. Song, B. Song, C. H. Cho, S. K. Lim and S. M. Jeong, *Mater. Today*, 2020, **32**, 46–58.
12 H. W. Choi, D. W. Shin, J. Yang, S. Lee, C. Figueiredo, S. Sinopoli, K. Ullrich, P. Jovancic, A. Marrani, R. Momentè, J. Gomes, R. Branquinho, U. Emanuele, H. Lee, S. Bang, S. M. Jung, S. Han, S. Zhan, W. Harden-Chaters, Y. H. Suh, X. Fan, T. H. Lee, M. Chowdhury, Y. J. Choi, S. Nicotera, A. Torchia, F. M. Moncunill, V. G. Candel, N. Duraes, K. Chang, S. Cho, C. H. Kim, M. Lucassen, A. Nejim, D. Jiménez, M. Springer, Y. W. Lee, S. Cha, J. I. Sohn, R. Igreja, K. Song, P. Barquinha, R. Martins, G. A. J. Amaratunga, L. G. Occhipinti, M. Chhowalla and J. M. Kim, *Nat. Commun.*, 2022, **13**, 814.
13 Y. J. Song, J. W. Kim, H. E. Cho, Y. H. Son, M. H. Lee, J. Lee, K. C. Choi and S. M. Lee, *ACS Nano*, 2020, **14**, 1133–1140.
14 C. Wang, X. Jiang, P. Cui, M. Sheng, X. Gong, L. Zhang and S. Fu, *ACS Appl. Mater. Interfaces*, 2021, **13**, 12313–12321.
15 Z. Zhang, X. Shi, H. Lou, X. Cheng, Y. Xu, J. Zhang, Y. Li, L. Wang and H. Peng, *J. Mater. Chem. C*, 2018, **6**, 1328–1333.

16 Z. Zhang, L. Cui, X. Shi, X. Tian, D. Wang, C. Gu, E. Chen, X. Cheng, Y. Xu, Y. Hu, J. Zhang, L. Zhou, H. Fong, P. Ma, G. Jiang, X. Sun, B. Zhang and H. Peng, *Adv. Mater.*, 2018, **30**, 1800323.
17 P. Li, Z. Sun, R. Wang, Y. Gong, Y. Zhou, Y. Wang, X. Liu, X. Zhou, J. Ouyang, M. Chen, C. Hou, M. Chen and G. Tao, *Front. Optoelectron.*, 2022, **15**, 151–157.
18 G. Liang, M. Yi, H. Hu, K. Ding, L. Wang, H. Zeng, J. Tang, L. Liao, C. Nan, Y. He and C. Ye, *Adv. Electron. Mater.*, 2017, **3**, 1770052.
19 C. Yang, S. Cheng, X. Yao, G. Nian, Q. Liu and Z. Suo, *Adv. Mater.*, 2020, **32**, 2005545.
20 T. Sun, F. Xiu, Z. Zhou, C. Ban, T. Ye, Y. Ding, J. Liu and W. Huang, *J. Mater. Chem. C*, 2019, **7**, 1472–1476.
21 Z. Zhang, K. Guo, Y. Li, X. Li, G. Guan, H. Li, Y. Luo, F. Zhao, Q. Zhang, B. Wei, Q. Pei and H. Peng, *Nat. Photonics*, 2015, **9**, 233–238.
22 B. O'Connor, K. H. An, Y. Zhao, K. P. Pipe and M. Shtein, *Adv. Mater.*, 2007, **19**, 3897–3900.
23 S. U. Kong, Y. Jeon, H. S. Lee, Y. H. Hwang, J. Chang, H. Kim, C. Y. Kim and K. C. Choi, *Adv. Opt. Mater.*, 2023, **11**, 2203130.
24 Z. Zhang, Q. Zhang, K. Guo, Y. Li, X. Li, L. Wang, Y. Luo, H. Li, Y. Zhang, G. Guan, B. Wei, X. Zhu and H. Peng, *J. Mater. Chem. C*, 2015, **3**, 5621–5624.
25 D. Zhou, D. Liu, G. Pan, X. Chen, D. Li, W. Xu, X. Bai and H. Song, *Adv. Mater.*, 2017, **29**, 1704149.
26 W. Xu, J. Liu, B. Dong, J. Huang, H. Shi, X. Xue and M. Liu, *Sci. Adv.*, 2023, **9**, eadi7931.
27 L. Zhang and M. J. Yuan, *Light: Sci. Appl.*, 2022, **11**, 736–738.
28 H. Song, Y. J. Song, J. Hong, K. S. Kang, S. Yu, H. E. Cho, J. H. Kim and S. M. Lee, *npj Flex. Electron.*, 2022, **6**, 66.
29 Y. H. Hwang, B. Noh, J. Lee, H. S. Lee, Y. Park and K. C. Choi, *Adv. Sci.*, 2022, **9**, 2104855.
30 D. Hu, X. Xu, J. Miao, O. Gidron and H. Meng, *Materials*, 2018, **11**, 184.
31 G. Li, F. Sun, S. Zhao, R. Xu, H. Wang, L. Qu and M. Tian, *Nano Lett.*, 2023, **23**, 8436–8444.
32 H. Mi, L. Zhong, X. Tang, P. Xu, X. Liu, T. Luo and X. Jiang, *ACS Appl. Mater. Interfaces*, 2021, **13**, 11260–11267.
33 D. Liu, J. Ren, J. Wang, W. Xing, Q. Qian, H. Chen and N. Zhou, *J. Mater. Chem. C*, 2020, **8**, 15092–15098.
34 J. Zou, X. Xie, Z. Zhou, X. Dong, Y. Wu, D. Zhang, M. Wang, C. Chen, F. Xiu and J. Liu, *J. Mater. Chem. C*, 2022, **10**, 12582–12587.
35 E. Bringuier, *J. Appl. Phys.*, 1990, **67**, 7040–7044.
36 X. Zhang and F. Wang, *APL Mater.*, 2021, **9**, 030701.
37 M. Bredol and H. S. Dieckhoff, *Materials*, 2010, **3**, 1353–1374.
38 T. Tokuno, M. Nogi, M. Karakawa, J. T. Jiu, T. T. Nge, Y. Aso and K. Suganuma, *Nano Res.*, 2011, **4**, 1215–1222.
39 J. Jiu, M. Nogi, T. Sugahara, T. Tokuno, T. Araki, N. Komoda, K. Suganuma, H. Uchida and K. Shinozaki, *J. Mater. Chem.*, 2012, **22**, 23561–23567.
40 Y. Zuo, X. Shi, X. Zhou, X. Xu, J. Wang, P. Chen, X. Sun and H. Peng, *Adv. Funct. Mater.*, 2020, **30**, 2005200.